Dynamical behavior of a system with three-spin interactions induced by a strong rf field

V. E. Zobov and M. A. Popov

L. V. Kirenskii Institute of Physics, Siberian Department, Russian Academy of Sciences, Novosibirsk
(Submitted 12 December 1992)
Zh. Eksp. Teor. Fiz. **103**, 2129–2141 (June 1993)

The dynamical behavior of the nuclear spin system of a crystal immersed in strong dc and cw rf magnetic fields is investigated. The study focuses on how the relaxation properties of the magnetization orthogonal to the effective field, and the ratio of the two- to three-spin dipole–dipole interactions in the average Hamiltonian, change as the orientation of this field changes in a rotating system of coordinates. The third and fourth moments of the NMR spectrum are determined in the rotating system of coordinates and used to calculate the free precession decay using the memory-function method. The relation between the three-spin interaction and the properties of free precession decay observed experimentally under magic-angle conditions and for angles other than the latter is clarified.

Although interactions whose elementary operations involve the participation of more than two spins are well-known in the theory of magnetism,[1] the dynamical properties of systems with such interactions remain practically unstudied. For this reason, it is interesting to study the behavior of spin systems in strong constant (H_0) and rf magnetic fields when the spin dynamics are determined by multispin average (effective) Hamiltonians.[2] Historically, the first and best-studied systems of this kind involve interaction with a cw rf field.[3–6] In these systems, a constant effective field acts on the spins in the rotating system of coordinates with a value $\omega_e=(\omega_1^2+\Delta^2)^{1/2}$ (where ω_1 is the rf field amplitude and Δ is its detuning from the Larmor frequency γH_0). This field makes an angle $\theta=\arctan(\omega_1/\Delta)$ with the direction of the field H_0. When ω_e greatly exceeds the average local field (ω_{loc}) due to dipole–dipole interactions, the motion of the spins averaged over rapid oscillations is studied in a doubly rotating system of coordinates (where the second rotation around the effective field takes into account the frequency shift due to the first moment of the effective interaction[3,5]). This motion is described by the effective Hamiltonian[3]

$$\mathcal{H}=\mathcal{H}_2+\mathcal{H}_3, \tag{1}$$

where

$$\mathcal{H}_2=m\sum_{i\neq j} b_{ij}[I_i^zI_j^z-(I_i^xI_j^x+I_i^yI_j^y)/2], \tag{2}$$

$$\mathcal{H}_3=(9/16\omega_e)\sum_{i\neq j\neq l}\{-2cb_{ij}b_{il}I_i^zI_j^zI_l^z+[c(b_{il}b_{lj}+b_{ij}b_{jl})-sb_{ij}b_{il}](I_j^xI_l^x+I_j^yI_l^y)I_i^z\}, \tag{3}$$

$$b_{ij}=\gamma^2\hbar(1-3\cos^2\theta_{ij})/2r_{ij}^3,$$

$$m=(3\cos^2\theta-1)/2,\quad c=\sin^2 2\theta,\quad s=\sin^4\theta.$$

Here θ_{ij} is the angle the internuclear vector $\mathbf{r}_{ij}$ makes with the magnetic field $\mathbf{H}_0$, and $\{I_i^x,I_i^y,I_i^z\}$ are the components of the vector spin operator at the lattice site i in a system of coordinates with the z-axis directed along the effective field.

By varying the amplitude and detuning of the rf field, we can vary the direction of the effective field, and accordingly the form of the Hamiltonian (1). For $\theta=0$ we are left with only the two-spin Hamiltonian arising from truncation of the dipole–dipole interactions; conversely, for the so-called "magic angle"

$$\theta=\theta_M=\arccos(1/\sqrt{3})=54°44' \tag{4}$$

only the three-spin interaction (3) remains. By choosing more complicated rf interactions, e.g., in the form of multipulse trains,[2] we can obtain effective Hamiltonians with interactions that are higher order in the number of spins. In many cases, these multispin interactions, which are proportional to powers of the small quantity $\omega_{\text{loc}}/\omega_e$, are all smaller in magnitude than the original dipole–dipole interaction. A fundamental practical goal of experiments involving strong rf fields is to eliminate the dipole–dipole interaction and thereby obtain high-resolution spectra in solids. However, an equally important scientific result of these experiments is that they allow us to study the dynamics of systems with multispan interactions.

The time dependence of the components of magnetization observed in CaF_2 in a strong cw rf field[3,4,6] differs qualitatively from the dependence observed when $\omega_1=0$.[7,8] In the absence of an rf field ($\theta=0$), the magnitude of the magnetization directed along the x-axis of the rotating system of coordinates decreases, passing through zero and once again increasing in the opposite direction; this leads to an oscillatory decay of the free precession that is well-known both experimentally[7,8] and theoretically.[7,9–12] In a strong rf field, the magnetization in the doubly rotating system of coordinates varies in both magnitude and direction.[4,13] In the experiments of Refs. 3 and 6, the authors observed relaxation of the magnitude of the magnetization. It was noted[6] that for $0<\theta<\theta_M$ the value of the free precession decay signal at the minima of the oscilla-

 1063-7761/93/061062-08$10.00 © 1993 American Institute of Physics

tions does not reach zero. At the magic angle (4) the free precession decay signal decays monotonically, without oscillations,[3,6] and for sufficiently long times is described by a simple exponential. The authors of Ref. 3 postulated the following empirical formula for the ω_e—dependence of the time constant in the exponent:

$$(T_2\omega_e)^{-1}=C_1M_2^0\omega_e^{-2}+2C_2q_1/3, \tag{5}$$

where

$$M_2^0=(3/2)^2N^{-1}\sum_{i\neq j}b_{ij}^2 \tag{6}$$

is the second moment of the NMR absorption line shape,[7] $C_1=0.28$, and the second term is due to nonuniformity of the field ω_e. It is interesting to note that the result $T_2=135$ μs obtained in Ref. 6 for $\omega_e=100$ kHz and $\mathbf{H}_0\|$ [100] also agrees with (5).

It is natural to postulate the existence of a connection between the observed features of free precession decay and the appearance of three-spin interactions in the Hamiltonian (1) under the experimental conditions.[1)] The results of existing theories do not answer this question. The first and second moments of the NMR spectrum were investigated in Refs. 3, 5, and 14 in a rotating system of coordinates, and Antonov *et al.*[15] obtained approximate expressions for $\theta=\theta_M$ in the doubly rotating system of coordinates for only one of the two magnetization components required to calculate the experimentally observed free precession decay.[3,6] One of the goals of this paper is to establish a connection between the features of free precession decay and the three-spin interactions.[2)] To this end, we will investigate theoretically the dynamics of a spin system with Hamiltonian (1) at arbitrary angles θ.

The relaxation of the component of the magnetization orthogonal to the effective field in the doubly rotating system of coordinates is given by the correlation function

$$M_+(t)=\mathrm{Sp}\{I^+(t)I^-\}/\mathrm{Sp}\{I^+I^-\},\quad I^\pm=I^x\pm iI^y, \tag{7}$$

whose real and imaginary parts give the projections of the magnetization

$$\begin{aligned}M_x(t)&=\mathrm{Sp}\{I^x(t)I^x\}/\mathrm{Sp}\{(I^x)^2\},\\ M_y(t)&=\mathrm{Sp}\{I^y(t)I^x\}/\mathrm{Sp}\{(I^x)^2\}.\end{aligned} \tag{8}$$

The time dependence of the operators is determined in the usual way:

$$I^\alpha(t)=\exp(i\mathscr{H}t)I^\alpha\exp(-i\mathscr{H}t).$$

The quantity $M_x(t)$ is an even function of time, while $M_y(t)$, which vanishes at $\theta=0$ because of $\mathscr{H}_3$, is an odd function of time. In fact, when we replace t by $-t$ in (8), we obtain after a cyclic permutation of the operators under the trace sign

$$M_y(-t)=\mathrm{Sp}\{I^x(t)I^y\}/\mathrm{Sp}\{(I^x)^2\}.$$

A final rotation of 90° around the z-axis, which does not change the axisymmetric Hamiltonian (1), yields the expression

$$M_y(-t)=-M_y(t).$$

For small times, the behavior of $M_+(t)$ is described by the following power series

$$M_+(t)=\sum_{n=0}^{\infty}M_n(it)^n/n!, \tag{9}$$

where

$$M_n=\mathrm{Sp}\{[\mathscr{H},\ldots[\mathscr{H},\underbrace{I^+]\ldots]}_{n}I^-/\mathrm{Sp}\{I^+I^-\}. \tag{10}$$

The coefficients (10) are the nth moments[7] of the spectral density, which is connected with $M_+(t)$ by a Fourier transform.

The second moment was found previously.[3,5,14] For the third moment we obtain the following expression when $I=1/2$:

$$\begin{aligned}M_3(\theta)&=M_3^{DE}+M_3^{EE},\\ M_3^{DE}&=-3\cdot4^{-1}Km^2(M_2^0)^{3/2}\{2cP_1+(3c-s)P_2\},\\ M_3^{EE}&=-4^{-4}K^3(M_2^0)^{3/2}\{(31c^3-3c^2s-3cs^2+s^3)L_1\\ &\quad+3(49c^3-13c^2s-cs^2+s^3)L_2+6c(9c^2-5cs+s^2)\\ &\quad\times(L_3+L_4)+6(29c^3-25c^2s+5cs^2-s^3)L_5\\ &\quad+12c(2c^2-2cs+s^2)L_6\}.\end{aligned} \tag{11}$$

Here $K^2=M_2^0\omega_e^{-2}$, and we introduce the following lattice sums:

$$\begin{aligned}L_1&=(B^3N)^{-1}\sum b_{ij}^2b_{ik}^2b_{il}^2,\quad L_2=(B^3N)^{-1}\sum b_{ij}^2b_{il}^2b_{kj}b_{ki},\\ L_3&=(B^3N)^{-1}\sum b_{ij}^2b_{il}^2b_{kj}b_{kl},\\ L_4&=(B^3N)^{-1}\sum b_{ik}^2b_{ij}b_{jk}b_{il}b_{kl},\\ L_5&=(B^3N)^{-1}\sum b_{il}^2b_{ik}b_{ij}b_{jk}b_{kl},\\ L_6&=(B^3N)^{-1}\sum b_{ij}b_{ik}b_{il}b_{jk}b_{kl}b_{lj},\\ P_1&=(B^2N)^{-1}\sum b_{ij}^2b_{ik}^2,\quad P_2=(B^2N)^{-1}\sum b_{ij}^2b_{ik}b_{jk},\\ B&=N^{-1}\sum b_{ij}^2\ .\end{aligned} \tag{12}$$

In these expressions the summation is over all lattice site labels except those that coincide.

The numerical values of the lattice sums are given in Table I for a simple cubic lattice and three orientations of the magnetic field $\mathbf{H}_0$ with respect to the crystallographic axes. The values of B, P_1, P_2, L_1 are obtained from the results of Refs. 16 and 17; we calculated the remaining sums over spins surrounding a particular spin within a cube with dimension equal to ten lattice constants. Refining the values of the sums by enlarging this cube affects

TABLE I. Numerical values of the lattice sums required to calculate $M_3(\theta)$.

Lattice sum	$H_0 \parallel [100]$	$H_0 \parallel [110]$	$H_0 \parallel [111]$
P_1	0,7977	0,891	0.955
P_2	0,0915	0,169	0.13
L_1	0,5040	0,708	0,916
L_2	0,072	0,142	0,129
L_3	−0,034	0,015	0,043
L_4	0,019	0,035	0,055
L_5	$2{,}0\cdot10^{-4}$	0,012	$3{,}8\cdot10^{-3}$
L_6	$-4{,}2\cdot10^{-4}$	$7{,}5\cdot10^{-3}$	−0,018

only the last decimal place. This estimate of the convergence of the lattice sums is inferred from their dependence on the number of sites in the lattice included in the calculation (Table II).

For convenience in later analysis, we give here the expression for the second moment written using the same notation:

$$M_2(\theta)=M_2^E+M_2^D,$$
$$M_2^E=2^{-5}K^2M_2^0\{(10c^2-4cs+s^2)P_1 + (19c^2-10cs+s^2)P_2\}, \quad (13)$$
$$M_2^D=m^2M_2^0.$$

It follows from Table I that the lattice sums with loops arising from the couplings P_2, L_2-L_6, are considerably smaller in magnitude than those without loops, which involve P_1 and L_1. The difference is enhanced for model lattices with higher dimensionality d (Ref. 18), for which we find in the limit $d\to\infty$

$$P_1=L_1=1, \quad P_2=0, \quad L_n=0, \quad n=2\text{–}6. \quad (14)$$

Figure 1 illustrates the influence of sums with loops on the ratio

$$\varepsilon=-M_3(\theta)/M_2^{3/2}(\theta), \quad (15)$$

as we go from $d=\infty$ to $d=3$. The differences are insignificant, but the simplifications in the computational procedure for the moments are appreciable; therefore, we will compute the fourth moment using this approximation. Since the remaining lattice sums are given by powers of the sum B, for M_4 we obtain a rather simple final expression

$$M_4(\theta)=M_4^{EE}+M_4^{ED}+M_4^{DD}, \quad (16)$$
$$M_4^{DD}=7m^4(M_2^0)^2/3,$$
$$M_4^{ED}=m^2K^2(M_2^0)^2(512c^2-75cs+29s^2)/144,$$
$$M_4^{EE}=4^{-5}K^4(M_2^0)^2(344.5c^4-176c^3s+105.5c^2s^2 - 28cs^3+6s^4).$$

The dependence of the ratio

TABLE II. Numerical values of the sums L_nB^3 entering into (12) obtained by summing over the $(2l+1)^3-1$ sites of a cube with an individual spin in the center. The values of the sums are given in the units $(\gamma^2\hbar/2r_c^3)^6$, where r_c is the distance between nearest neighbors.

l	L_1B^3	L_2B^3	L_3B^3	L_4B^3	L_5B^3	L_6B^3
			$H_0 \parallel [100]$			
1	957,0	61,9	−148,0	37,05	−4,26	2,482
2	1140,0	150,2	−99,9	41,79	−2,24	−1,326
3	1178,0	165,1	−87,3	44,46	−0,26	−1,020
4	1190,1	169,7	−83,2	45,35	0,27	−1,011
5	1195,1	171,6	−81,6	45,73	0,48	−1,012
			$H_0 \parallel [110]$			
1	63,92	8,22	−3,80	1,400	0,400	0.9069
2	84,47	15,77	−0,06	3,663	1,150	0,9603
3	89,05	17,52	1,25	4,230	1,404	0,9798
4	90,54	18,10	1,71	4,418	1,492	0,9811
5	91,15	18,35	1,90	4,497	1,530	0,9813
			$H_0 \parallel [111]$			
1	5,54	0,309	−0,094	0,297	−0,0208	−0,1285
2	9,13	1,127	0,196	0,545	0,0120	−0,2037
3	10,01	1,418	0,399	0,624	0,0314	−0,2115
4	10,30	1,522	0,482	0,653	0,0411	−0,2125
5	10,42	1,567	0,519	0,665	0,0460	−0,2128

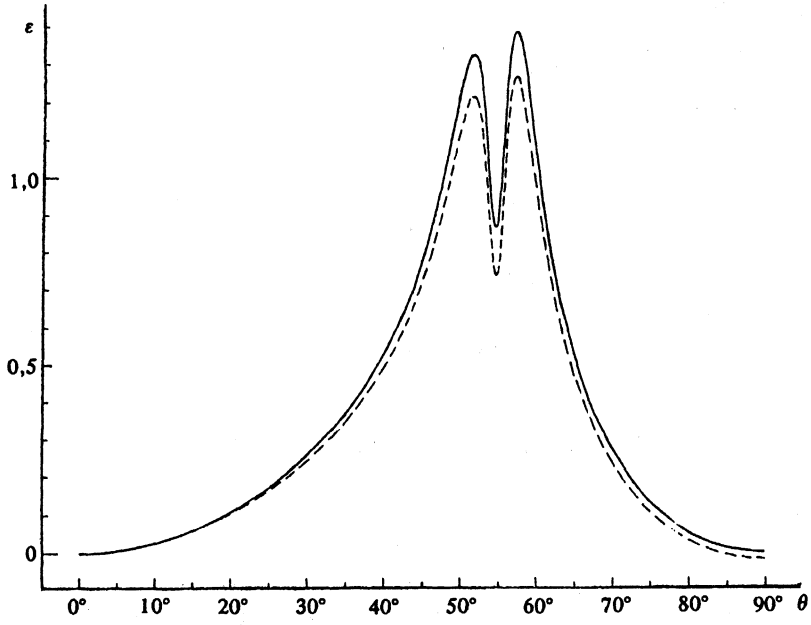

FIG. 1. Dependence of the normalized third moment ε on the orientation of the effective field for a three-dimensional cubic lattice with $H_0 \| [100]$ (dashed curve) and for an infinite-dimensional lattice (solid curve).

$$\mu = M_4(\theta)/M_2^2(\theta) \tag{17}$$

on θ calculated using Eq. (16) is shown in Fig. 2. In particular, for $\theta=\theta_M$ we have $\mu=4.1102$, $\varepsilon=0.8616$.

Approximating the interaction by one with infinite radius (r_0), for which the sums with loops and without loops become equal in magnitude, leads to a still greater simplification.[19] Unfortunately, the properties of a system in the limit $r_0 \to \infty$ deviate much farther from those of a three-dimensional lattice with finite r_0 than is the case for a system in the limit $d \to \infty$.

In Figs. 1 and 2, we note the presence of sharp minima in ε and μ for $\theta=\theta_M$. They are caused by the disappearance of contributions from the mixed terms M_3^{ED} and M_4^{ED} due to the combined action of $\mathscr{H}_2$ and $\mathscr{H}_3$, which in turn is due to vanishing of $\mathscr{H}_2$ when $\theta=\theta_M$.

Let us turn to an analysis of the behavior of $M_+(t)$ at large times. We make use of the method of memory functions,[2,9] and write the equation for $M_+(t)$ in the form

$$\frac{d}{dt} M_+(t) = -\int_0^t G(t-t') M_+(t') dt'. \tag{18}$$

This integral equation is exact if we know the exact expression for its kernel, i.e., the memory function $G(t)$. However, finding this kernel is as complicated a problem as finding the correlation function (7) itself. The advantage to this method is that qualitatively correct results are already obtained when $G(t)$ is chosen in the form of a simple function. For example, a Gaussian function

$$G_r(t) = M_2 \exp\{-(\mu-1)M_2 t^2/2\} \tag{19}$$

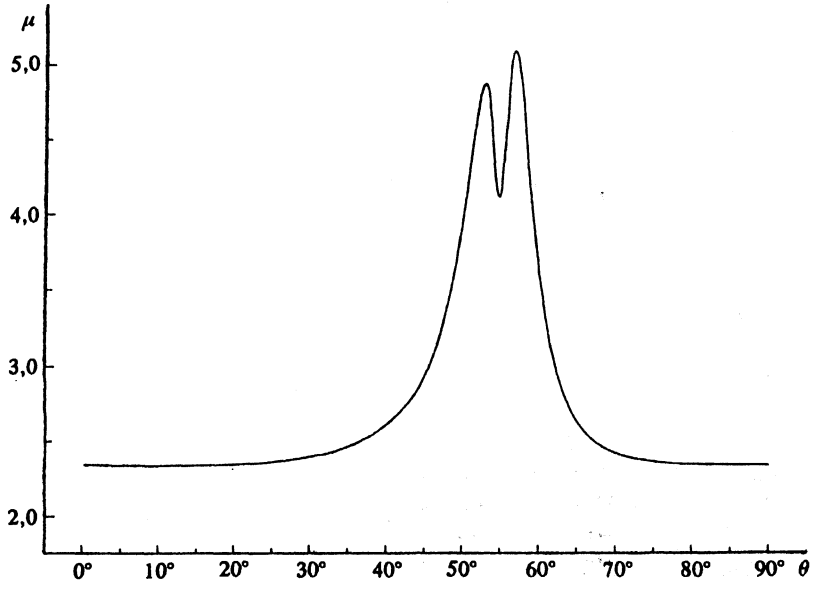

FIG. 2. Dependence of the normalized fourth moment μ on the orientation of the effective field.

was successfully used in Refs. 2, 9, and 10 for a system with two-spin interactions. Since in our case the odd moments are also nonzero, the memory function should contain, in addition to (19), an imaginary part, which we choose in the form

$$G_i(t) = -itM_2^{1/2}\varepsilon G_r = (t). \tag{20}$$

We call the reader's attention to the fact that by using the dependence of the parameters on the moments given in (19) and (20) we ensure a solution to Eq. (18) that involves the required values of the moments M_2, M_3, and M_4.

The Laplace transform of the solution to Eq. (18) has the form

$$M_+(z) = 1/[z + G_r(z) + iG_i(z)], \tag{21}$$

where z is the transform parameter, and $G_r(z)$ and $G_i(z)$ are the transforms of the real and imaginary parts of the memory function:

$$G_r(z) = M_2\pi^{1/2}[2(\mu-1)M_2]^{-1/2}\exp(\tilde{z}^2)\operatorname{erfc}(\tilde{z}), \tag{22}$$

$$G_i(z) = \varepsilon M_2^{1/2}\frac{d}{dz}G_r(z), \quad \tilde{z} = z[2(\mu-1)M_2]^{-1/2}.$$

Expression (21) allows us to compute and study the shape of the NMR spectrum in the rotating system of coordinates for various angles θ. For now, however, we limit ourselves to using it to obtain the characteristics of the long-time portion of the free precession decay for angles θ close to the magic angle, which are the best-studied experimentally.[3,6] For this it is necessary to find the zero of the denominator (21) that is closest to the coordinate origin, as was done, e.g., in Ref. 20 for the special case $\varepsilon = 0$.

For $\theta \approx \theta_M$, the memory function decays much more rapidly than the function $M_+(t)$, which for coordinates close to the zero z_0 implies $|z_0|^2 \ll 2(\mu-1)M_2$, so that it can be found with sufficient precision by saving a few of the leading terms in the expansion for the error function appearing in (22) in powers of $\tilde{z}$. To within quadratic terms in (21), we have

$$\tilde{z}_0 = \tilde{z}_r + i\tilde{z}_i,$$

$$\tilde{z}_r = \{R_r/2 + [\tilde{\varepsilon}(\tilde{\varepsilon}-R_i) + 2 - \mu]/\pi^{1/2}\}/(1 + 4\tilde{\varepsilon}^2/\pi), \tag{23}$$

$$\tilde{z}_i = \{(R_i - \tilde{\varepsilon})/2 + \tilde{\varepsilon}[R_r/\pi^{1/2} + 2(2-\mu)/\pi]\}/$$
$$(1 + 4\tilde{\varepsilon}^2/\pi),$$

where $\tilde{\varepsilon} = \varepsilon[2/(\mu-1)]^{1/2}$, and R_r and R_i are the real and imaginary parts of the square root of

$$4(\mu-2)^2/\pi - 4 + \tilde{\varepsilon}^2(8/\pi - 1) + i4\tilde{\varepsilon}(\mu+1)/\pi^{1/2}.$$

For $\theta = \theta_M$, after substituting the values of ε and μ we find

$$\tilde{z}_r = -0.27, \quad \tilde{z}_i = 0.30. \tag{24}$$

The oscillation frequency of the function $M_+(t)$ is given by $\tilde{z}_i$, while the damping rate is given by $\tilde{z}_r$. In particular, for the constant C_1 in (5) we obtain

$$C_1 = -\tilde{z}_r[2(\mu-1)]^{1/2}[M_2/M_2^0K^2]^{1/2} = 0.30. \tag{25}$$

Here the numerical value follows from exact values of M_2, M_2^0, and K^2 for the second expression under the radical. The calculated value of C_1 is in good agreement with the experimental value (5).

Relation (23) allows us to track the influence of the parameter ε. For example, when ε is equal to zero we have $\tilde{z}_r = -0.54$, i.e., the rate of attenuation increases by a factor of two.

We note finally that the constant C_1 is independent of ω_e because of the disappearance of the term $\mathscr{H}_2$ in (1) at $\theta = \theta_M$. Expression (3) for $\mathscr{H}_3$ has the form of a scale factor, which implies $M_n \propto \omega_e^{-n}$, $T_2 \propto \omega_e$, and also that μ and ε are independent of ω_e. When the orientation deviates from its magic value, the dependence of the attenuation on ω_e is more complicated; however, it can still be found by substituting the expressions for ε and μ determined above for arbitrary angles θ into Eq. (23).

A more complete picture of the behavior of $M_+(t)$ for various orientations of the effective field is shown in Fig. 3, where the results of a numerical solution of Eq. (18) with the kernel (19) and (20) are presented. In the numerical solution, the time interval under investigation was subdivided into 1000 parts.

We now make a few changes in the memory function. It is natural to expect that at after a sufficiently long time the memory function, like the free precession decay (Refs. 3, 6, and 8), is best described by a simple exponential rather than a Gaussian. In particular, local field fluctuations can produce such a change. A function possessing this property, e.g., the function proposed by Anderson[21] to explain the exchange narrowing of the spectra, can be used if we change its coefficients in the following way:

$$G_r(t) = M_2 \exp\left\{-(\mu-1)M_2\int_0^t\int_0^{t_1} g(t_2)dt_2dt_1\right\}. \tag{26}$$

At small times [or for $g(t) \equiv 1$] (26) reduces to (19), while for $t \gg \tau_c$, where τ_c is the temporal scale of attenuation of $g(t)$, we have

$$G_r(t) = M_2 \exp\{-(\mu-1)M_2\tau_c t\}. \tag{27}$$

The solution to (18) obtained by replacing (19) with (27) in the real and imaginary parts of the memory function over the entire time interval is even simpler. The time dependence of $|M_+(t)|$, which was calculated for this case in Ref. 6 for $M_2^{1/2}\tau_c = 0.77$, has the same qualitative properties as shown in Fig. 3. Since the qualitative differences between these two limiting cases as expressed in the oscillation frequencies and attenuation rates of $|M_+(t)|$ are also insignificant, we have not carried out any calculations using the kernel (26).

The decaying amplitude of the rotating component of the magnetization is plotted for various angles θ in Fig. 3. As represented by the magnitude of the function $M_+(t)$,

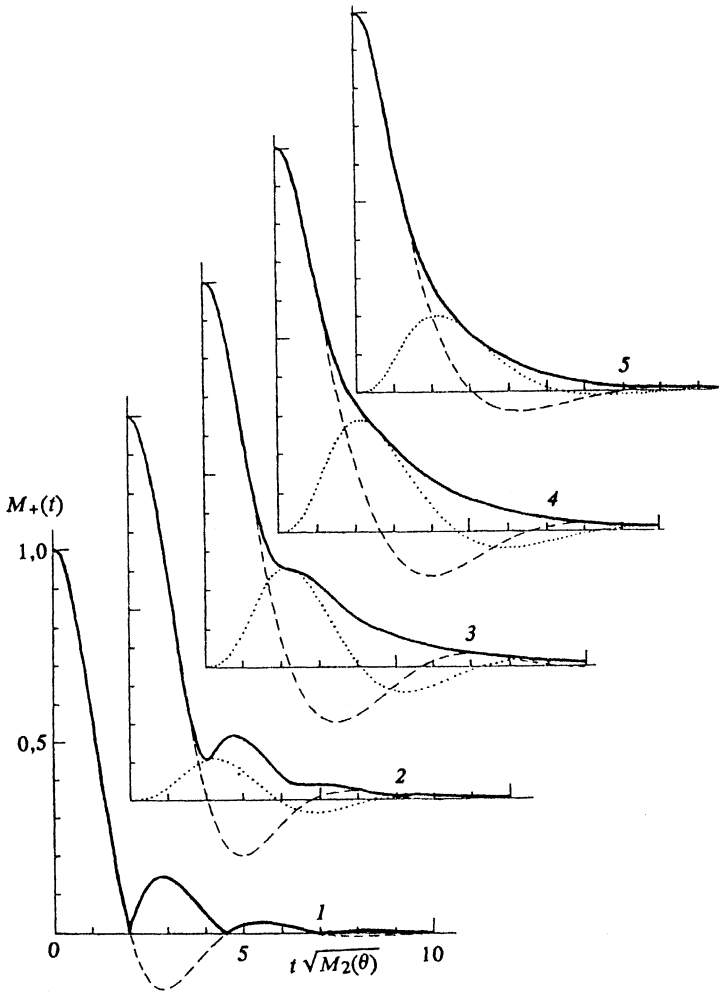

FIG. 3. Time dependence of the correlation function $M_+(t)$ (the absolute value of the function is the solid curve, the real part is the dashed curve, and the imaginary part is the dotted curve) for $\theta=0°$ (*1*), 30° (*2*), 45° (*3*), 50° (*4*), and $\theta=\theta_M=54.7°$ (*5*).

this quantity has the same behavior as the free precession decay observed experimentally and described at the beginning of this article, which thus confirms the connection between these features and the three-spin interaction. Furthermore, these results reveal the mechanism by which this interaction causes the specific changes in the free precession decay with increasing angle θ mentioned above. The oscillations in the magnitude of the magnetization rise above the zero line because $M_y(t)$ develops an imaginary part in $M_+(t)$ (Ref. 22) which does not vanish at the same time as the real part of $M_x(t)$, as the corresponding curves show in Fig. 3. Note that a change in the ratio of the imaginary and real parts implies a change in the direction of magnetization in the doubly rotating system of coordinates, which was mentioned in Refs. 4 and 13. The main reason that the oscillations in $|M_+(t)|$ disappear at the magic orientation (4) is an increase in the attenuation rate of the memory function, which is indicated by the growth in μ. The same results are obtained, according to (3), when an imaginary part characterized by the quantity ε appears in μ. In this case, the monotonic decrease in the value of $|M_+(T)|$ is accompanied by oscillatory behavior of $M_x(t)$ and $M_y(t)$ [see Fig. 3 and Eq. (23)]. However, these are no longer the oscillations in the component $M_x(t)$ that occur for $\theta=0$, which are connected with the change in the ordering from magnetization to two-spin correlations. At $\theta=\theta_M$ the oscillations between $M_x(t)$ and $M_y(t)$ are oscillations in the direction of the magnetization, whose rate is determined by the moment M_3, whereas for $\theta=0$ the oscillation rate is determined by the moments M_2 and M_4.

Thus, the theory given here allows us to explain the dynamics of spins in strong cw rf fields as observed in free precession decay signals in the rotating system of coordinates by relating these features to the presence of three-spin interactions in the average Hamiltonian.

Since the theory is in qualitative agreement with experiment, we may attempt to add quantitative refinements. These refinements are necessary because the experimentally observed increase in the free precession decay oscillations as the angle θ departs from θ_M is more rapid than is predicted by the theory given here (Fig. 3). The cause of this discrepancy is primarily the form we used for the kernel of the integral equation (18), in which we treated the combined action of $\mathscr{H}_2$ and $\mathscr{H}_3$ in an average way, which was unnecessary. A more detailed equation for the correlation functions could have been used as an alternative. In particular, we could have followed the treatment of the dipole–dipole interaction given in Refs. 11, 12, and 23 and derived an integral equation for $M_+(t)$. Let us do so here: in place of the zero-order approximation we introduce the function

$$M_+^{(z)}(t)=(1+iat)^{-1/2}$$

$$\times\exp\{-[a^2t^2+b^2t^2/(1+iat)-iat]/2\}, \quad (28)$$

where $a=cM_2^0/4\omega_e$, $b^2=4m^2M_2^0/9$. This expression is derived in the Appendix by keeping only interactions between the z-components of the spin in the Hamiltonian (1). The rotation of the spins in longitudinal local fields is distinguished[11,12,21,23] for a number of reasons, the most important of which is the axial symmetry of the Hamiltonian.

The result (28) was obtained using the approximation of a lattice of high dimension. For systems with infinite interaction radius,[19] the term $-a^2t^2/2$ is absent from the exponential, and the constant a increases by a factor of 3. The use of these two methods[18] for increasing the number of neighbors leads to forms of the functions $M_+^{(z)}(t)$ that differ even for the local field; this is one more property of the three-spin interaction.

Since $\mathscr{H}_3$ vanishes at $\theta=0$, the function (28) is converted to an ordinary Gaussian decay. At other angles it decays more slowly than a Gaussian function for the same moment M_2, and possesses all the properties derived from the Hamiltonian $\mathscr{H}_3$: odd moments, imaginary part, asymmetric spectra, etc. It is not difficult to see that the difference in the results for $\theta=0$ and $\theta=\theta_M$ is due to the fact that the Gaussian local field at an individual spin enters into $\mathscr{H}_3$ quadratically [see Eq. (A5)]. This simple example allows us to use the language of local fields to improve our understanding of how the two- and three-spin interactions differ. For clarity let us consider variations in the spectrum, which are easy to explain by writing $\mathscr{H}_3$ in the same form as $\mathscr{H}_2$ with interaction constants $\bar{\beta}_{0i}=\beta_{0i}h_0$ that depend on the local field (A4). For small local fields this constant decreases (the center of the spectrum rises), while for large fields it increases (the wings of the spectrum rise). When the sign of the field changes, the sign of the constants changes as well (i.e., the contribution of negative frequencies decreases, which leads to asymmetry in the spectrum).

In conclusion, the authors are grateful to A. E. Mefyod for drawing our attention to the experimental data long before publication, and to V. A. Atsarkin and the participants in his seminar for useful discussion of the results.

APPENDIX

Let us find the form of the correlation function (7) when only the interaction between the z-projections of the spins is retained in the Hamiltonian (1). In this case, the known properties of the creation operators allow us to write the time dependence of $I_0^+(t)$ in explicit form:

$$M_+^{(z)}(t)=\mathrm{Sp}\Big\{\prod_{i\neq j}\{\exp[it(qb_{0i}b_{0j}I_i^zI_j^z+mb_{0i}I_i^z)]$$

$$\times\exp[2itqb_{0i}b_{ij}I_i^zI_j^z]\}\Big\}, \quad (A1)$$

where $q=-9c/8\omega_e$. In (A1) we have identified contributions from terms for which the position of an individual spin "0" (the spin whose correlation function we wish to calculate) is at the edge or in the center of a chain of three coupled spins. We have chosen this description because the lattice properties of these contributions differ, a fact which we will use in subsequent transformations.

Let us transform (A1), using the properties of exponential operators for $I=1/2$:

$$\exp(2i\alpha I_i^z)=\cos\alpha+2iI_i^z\sin\alpha,$$
$$\exp(4i\beta I_i^zI_j^z)=\cos\beta+4iI_i^zI_j^z\sin\beta. \quad (A2)$$

For $\theta=0$, when $q=0$ we obtain the well-known result[7] for the decay in the form of a product of cosines. The appearance of a term involving the product of operators $I_i^zI_j^z$ before the sine when $\theta\neq0$, which is a consequence of the three-spin interaction, implies that we must sort out all possible types of pairing of the operators I_i^z that will lead to a nonzero value of the trace. Similar problems are well known from calculations of the partition function in the Ising model. The distinctive feature of Eq. (A1) is the presence of the fixed "0" site.

These problems can be overcome by using the high-dimensional lattice approximation after neglecting the contribution of terms that form loops made up of lattice bonds in the time series. Doing this leads to a term in (A1) with the sine of the second exponential when it is represented in the form (A2), and we discard it. Then we can remove the remaining factor in this exponent, which does not contain operators, from under the trace sign, i.e.,

$$\prod_{i\neq j}\cos(tqb_{0i}b_{ij}/2)\underset{d\to\infty}{=}\exp(-a^2t^2/2), \quad (A3)$$

and introduce the local field into the exponent of the first exponential in the remaining expression under the trace:

$$h_0=\sum_j b_{0j}I_j^z, \quad (A4)$$

which we write in the form

$$\exp\{it[mh_0+qh_0^2+a/2]\}. \quad (A5)$$

In the limit of a large number of neighbors, the distribution of the local field H_0 is given by a Gaussian function. Replacing the trace calculation in (A1) by an integration over this distribution function, we obtain the required Eq. (28) after calculating the integral.

In the limit of an infinite interaction radius, the difference between the two terms in (A1) disappears; therefore, the second exponential can be transformed in exactly the same way as the first.

[1)]The authors of Ref. 13 used a different approach, in which the motion of the spins was investigated under the combined action of the rf field and dipole–dipole interactions. The integral equations they derived are complicated even in the lowest-order approximation. Although this approach remains the only one possible in insufficiently strong rf fields, for $\omega_e\gg\omega_{\text{loc}}$ the transition to an average Hamiltonian allows the description of the spin dynamics to be simplified.

[2)]Preliminary results on this topic are given in Ref. 6.

[1] É. L. Nagaev, *Magnets with Compound Exchange Interactions* (in Russian), Nauka, Moscow, 1988.

[2]U. Heberlen and M. Mering, *High-resolution NMR in Solids* (in Russian), Mir, Moscow, 1980.
[3]M. Lee and W. I. Goldburg, Phys. Rev. A **140**, p. 1261 (1965).
[4]H. M. Einbinder and S. R. Hartmann, Phys. Rev. Lett. **17**, 518 (1966).
[5]A. E. Mefyod and V. A. Atsarkin, Zh. Eksp. Teor. Fiz. **74**, 720 (1978) [Sov. Phys. JETP **47**, 378 (1978)].
[6]A. E. Mefyod, A. V. Proslavtsev, V. E. Zobov *et al.*, Pis'ma Zh. Eksp. Teor. Fiz. **55**, 412 (1992) [JETP Lett. **55**, 418 (1992)].
[7]A. Abragam, *The Principles of Nuclear Magnetism*, Clarendon, Oxford, 1961.
[8]M. Engelsberg and I. J. Love, Phys. Rev. B **10**, 822 (1974).
[9]A. Abragam and M. Gold'man, *Nuclear Magnetism: Order and Disorder* (in Russian), Mir, Moscow, 1984, Part 1, Ch. 1.
[10]G. W. Parker and F. Lado, Phys. Rev. B **8**, 3081 (1973).
[11]G. Sauermann and M. Wiegand, Physica B **103**, 309 (1981).
[12]G. E. Karnaukh, A. A. Lundin, B. N. Provotorov, and K. T. Summanen, Zh. Eksp. Teor. Fiz. **91**, 2229 (1986) [Sov. Phys. JETP **64**, 1324 (1986)].
[13]D. Walgraef, Physica **63**, 527 (1973).
[14]O. F. Antonov and R. Kh. Sabirov, Phys. Status Solidi (b) **125**, K117 (1984).
[15]O. F. Antonov, E. R. Butkevich, and R. Kh. Sabirov, Izv. Vuzov. Radiofizika **28**, 2150 (1985).
[16]S. J. K. Jensen and E. K. Hansen, Phys. Rev. B **7**, 2910 (1973).
[17]H. T. Stokes and D. C. Ailion, Phys. Rev. B **15**, 1271 (1977).
[18]V. E. Zobov, Teor. Mat. Fiz. **77**, 426 (1988); Teor. Mat. Fiz. **84**, 111 (1990).
[19]V. E. Zobov, *Abstracts from the Proc. of the 12th All-Union School-Symp. on Magnetic Resonance* (in Russian), p. 9. Perm': Perm' University, 1991.
[20]V. Denner and M. Wagner, J. Chem. Phys. **81**, 5034 (1984).
[21]P. W. Anderson, J. Phys. Soc. Jpn. **9**, 316 (1954).
[22]V. E. Zobov, A. V. Ponomarev, and M. A. Popov, *Abstracts from the Proc. of the 12th All-Union School-Symp. on Magnetic Resonance* (in Russian), p. 10. Perm': Perm' University, 1991.
[23]A. A. Lundin, A. V. Makarenko, and V. E. Zobov, J. Phys.: Condensed Matter **2**, 10131 (1990).

Translated by Frank J. Crowne